LBL-34434
UC-404

Nonlinear Optical Response of Semiconductor Quantum Wells Under High Magnetic Fields

D.S. Chemla

Physics Department
University of California

and

Materials Sciences Division
Lawrence Berkeley Laboratory
University of California
Berkeley, CA 94720

July 1993

This work was supported by the Director, Office of Energy Research, Office of Basic Energy Sciences, Division of Materials Sciences, of the U.S. Department of Energy under Contract No. DE-AC03-76SF00098.

Nonlinear Optical Response of Semiconductor Quantum Wells Under High Magnetic Fields.

D.S. Chemla
Physics Department, University of California at Berkeley,
Material Sciences Division, Lawrence Berkeley Laboratory.

I). Introduction

In semiconductor quantum wells (QW) the electronic states have a reduced, quasi-2D dimensionality. This property alone results in a wealth of new physical properties and interesting applications in the field of electronics and photonics.[1] Motivated by this success, an intense research activity has been directed at further reducing the dimensionality of the electronic states to 1D and 0D. The numerous efforts to make semiconductor structures such has quasi-1D quantum wires and quasi-0D quantum boxes and micro-crystallites have, so far, failed to produce samples of quality comparable to that of the available QW's. Two major difficulties are encountered. They are related to i) the atomic control of size fluctuations, and ii) the control of surface and interface defects. For these reasons it is interesting to find alternative ways to explore the nonlinear optical properties of quasi-0D system while avoiding these practical difficulties. As shown below the dimensionality of the electronic states of semiconductor QW can be tuned continuously from quasi-2D to quasi-0D, in materials with excellent quality and uniformity by application of a magnetic field perpendicular to the QW.[2-6] Further interest in QW's under large magnetic field stems from the prediction of many-body theory, according to which in such systems and at thermodynamic equilibrium, an ensemble of spin polarized electron-hole pairs behave like a gas of non-interacting and non-polarizable point-like Bosons.[7,8] This two-component quantum system is expected

to exhibit new and interesting many-body properties.

In this article we review our recent investigations on the nonlinear optical response of semiconductor quantum wells in a strong perpendicular magnetic field, H. The paper is organized as follows. In Section II, we dicuss the evolution of the linear optical properties of GaAs QW's as a function of H and examine how the magneto-excitons (MX) extrapolate continously between quasi-2D QW excitons (X) when $H = 0$, and pairs of Landau levels (LL) when $H \rightarrow \infty$. In Section III, we present femtosecond time resolved investigations of their nonlinear optical response. We stress the evolution of MX-MX interactions with increasing H.[9,10] Finally in Section IV, we study how, as the dimensionality is reduced by application of H, the number of scattering channels is limited and relaxation of electron-hole pairs is affected.[11] We also discuss how nonlinear optical spectroscopy can be exploited to access the relaxation of angular momentum within magneto-excitons.[12]

II) Linear Optical Response of Magneto-excitons

The linear optical response of magneto-excitons has been extensively studied.[2-6] When a constant magnetic field is applied perpendicular to a QW, the wave function for the relative e-h coordinate, $r = r_e - r_h$, of pairs with zero center of mass momentun satisfies the effective-mass Schrödinger equation,

$$[\frac{1}{2m_e}(p + \frac{e}{2c}H\times r)^2 + \frac{1}{2m_h}(p - \frac{e}{2c}H\times r)^2 - \frac{e^2}{\varepsilon_o r}]\,\zeta_v(r) = E_v\zeta_u(r). \qquad (I)$$

The e-h pairs experience the total potential which consists of the sum of the quadratic-

potential imposed by H and the 1/r Coulomb potential,

$$V(r) = [(\frac{1}{2}\lambda r)^2 - \frac{2}{r}]R_y, \quad (2)$$

where R_y is the 3D-exciton Rydberg. The parameter λ measures the ratio between the magnetic and the Coulomb confinements as measured by the corresponding zero-point energies, $\lambda = \omega_c/2R_y$, where ω_c is the cyclotron frequency. It can also be expressed, $\lambda = (a_o/r_c)^2$, where the Bohr radius, a_o, measures the range of the Coulomb force and the cyclotron radius, r_c, characterizes the magnetic length. For $\lambda = 0$ the e-h pairs form usual quasi-2D excitons, $\zeta_\nu(r) \rightarrow \phi_\nu(r)$. For $\lambda \rightarrow \infty$ they tend toward e and h in Landau levels, $\zeta_\nu(r) \rightarrow L_\nu(r)$. For the intermediate values of λ, they form magneto-excitons. It is worth noting that when $r \rightarrow \infty$, $V(r) \rightarrow \infty$ for any non zero value of H. Hence, all the MX states originate from the **bound** states of the unperturbed X,[2,3] and can be labelled accordingly by the indices 1S, 2S, 3S etc...

The experimental linear absorption spectra of a high quality GaAs/AlGaAs-QW structure ($L_z = 84$Å) at low temperature, T = 4K, and in a perpendicular magnetic field, are shown in Figure 1. The spectra were measured with σ_- polarized light as H was tuned from H = 0 →12T. At the higest field where $r_c \simeq 71$Å, the magnetic confinement is significantly larger than the Coulomb confinement, $\lambda \simeq 4$. The transition from 2D behavior at low fields to 0D behavior at high fields and the evolution of the MX's from the bound 2D-X states are nicely displayed. On can see the small diamagnetic shift experienced by the lowest energy 1S heavy-hole (hh) and light-hole (lh) excitons. The higher energy MX's shift much faster as the H increases. They clearly start close to the hh-gap, which in this sample is approximately located at the lh-X energy, and tend

toward the LL's at high field. As the MX's separate away from the gap, the peak at the lh-X experiences a drop in oscillator strength. This demonstrate that when H = 0, the hh-X excited states in fact contributed to this peak but were not resolved. Figure 2 compares the 12T-linear absorption for σ_- (dashed line) and σ_+ (solid line). They are Zeeman-split in agreement with the QW selection rules at the Γ-point of the Brillouin zone which are shown in the inset of Figure (2). At such a high field the confinement is strong enough that the absorption strength is almost zero between the 1s and 2s MX, indicating that the MX's are almost diagonal in the LL basis. These spectra are in good agreement with the theoretical calculations of Ref.[6]. It is clearly seen how the oscillator strength is now concentrated in the sharp MX-peaks which directly reflect the quasi-0D density of states of the eh pairs.

II) Nonlinear Optical Response of Quasi-0D Magneto-excitons

Pump/probe experiments provide a very powerful technique to measure the nonlinear response of a medium. In time resolved experiments one uses a short, intense and relatively narrow pump to excite the sample. Its transmission is measured by a short but weak and broad band probe. The time resolution is obtained by varying the delay, Δt, between the pump and probe pulses. The experimental data is usually collected by measuring the difference between the probe transmission when the pump is applied and when it is not. Examples of the differential absorption spectra, or DAS, obtained by this method are presented below. In the case of semiconductors the most intuitive way of interpreting pump/probe experiments is to consider that the pump creates populations of excitons (or magneto-excitons in the presence of H) whose energy and angular momentum are determined by the pump-photon energy and polarization. The broad band

probe then measures the change of absorption induced by the presence of these populations. For excitation in the transparency region, below the gap, the populations are virtual and last only as long as the pump is present in the sample. For excitation above the gap, the populations are real and can relax after being generated. Exciton populations affect the absorption through several mechanisms.[1] Charge density effects (collisional broadening and Debye screening) are independent of the angular momentum, but other processes such as phase space filling (PSF), exchange (EXCH) and exciton-exciton interaction (XXI) depend critically on the spin.[1] As the time delay is changed, the dynamics of these effects cand be followed on the variations of the DAS vs Δt.

In several theoretical articles,[7,8,13-15] it was shown that in the extreme magnetic limit and for a symmetric e-h system, ($V_{ee} = V_{hh} = -V_{eh}$), the ground state energy of an MX gas is just the sum of the energies of the individual MX's. This result implies that at high H the MX-MX interaction disappears. It can be explained intuitively, in a way which captures the essence of the exact many-body theory. For pure parabolic bands (neglecting the Coulomb interaction), the electron and hole wavefunctions depend only on r_c and are, therefore, mass independent. As H is increased the magnetic confinement dominates the Coulomb interaction, and the e and h are forced into almost identical and overlapping wavefunctions. Hence the quasi-0D MX's occupy much smaller volume at high field and, for the same density, show much less PSF. Furthermore, as the magnetic potential, $(\lambda r/2)^2$, increases it restricts more and more e's and h's on top of one another making the MX's more rigid and locally neutral and therefore much less polarizable. For exactly symmetric e-h system, $V_{ee} = V_{hh} = -V_{eh}$, this results in a perfect cancellation of the MX-MX interaction. XXI manifests itself directly as a blue shift of the 1shh-X peak

induced by a population of 1shh-X. This shift can be interpreted as a hard core repulsion which measures the extra energy cost necessary to create an 1shh-X in the presence of other 1shh-Xs.[16] It has been clearly resolved at H = 0 during resonant pumping of 1shh-X or subsequent to the formation of 1shh-X after excitation of e-h pairs in the continuum.[17,18] At low and moderate X-densities the blue shift is proportional to the XXI repulsive potential and to the X-density.[16-18]

High density optical nonlinear effects are shown in Figure (3a) and (3b), where we present the DAS, seen by a σ_--probe for excitation resonant with the lowest 1S-hh MX ($\omega \simeq 1.56$eV) with respectively a σ_--pump and a σ_+-pump, of the same intensity. Very strong responses are observed at photon energies up to $\omega = 1.67$eV. As previously explained, two types of nonlinearities, spin-dependent and spin-independent, contribute to the DAS. The pump/probe technique is actually able to separate spin-dependent nonlinearities from the spin-independent ones. This is shown in Figure (3c) where the spectra of Figure (3a) are substrated from those of Figure (3b). One clearly sees that in this difference all the nonlinear response above $\omega \simeq 1.59$eV disappears, demonstrating that the high energy MX's (2s and above) are only sensitive to the charge density effects (collisional broadening and dielectric screening) induced by the resonantly excited 1shh–σ_--MX's or 1shh–σ_+-MX's. The same figure clearly shows that the 1s-MX's ($\omega < 1.59$eV) on the contrary, are very sensitive to the spin of the MX's created by the pump. This behavior is detailed in Figure (4), where we compare an expanded part of the lower portion of the absorption spectra seen by a σ_--probe at H = 0T and H = 12T, for $\Delta t = -660$fs, 0fs and +660fs after excitation by a σ_--pump and a σ_+-pump. At $\Delta t = -660$fs the spectra are essentially that of the unexcited sample. For pump and probe

both σ_- polarized, the 1sh-MX response is an instantaneous gain and the blue shift at $\Delta t = 0$, which evolves toward a strong saturation and a smaller blue shift at $\Delta t = 660$fs. This is due to phase space filling (PSF) and exchange (EXCH) by the coherent ($\Delta t = 0$) and then the relaxed ($\Delta t = 660$fs) 1shh–σ_--MX's created by the pump. The difference between the H = 0T and the H = 12T cases is only qualitative. The high field effects are similar to the low field ones, but significantly attenuated. The instantaneous blue shift changes from 1.9meV → 0.3meV. Since the 1shh and 1slh originate from distinct e and h states, the 1slh response is not due to PSF and EXCH produced by the real 1shh MX's. It comes from the pump induced virtual-populations of 1slh, i.e. the AC-Stark Effect.[1] When the pump polarization is reversed to σ_+, the 1shh–σ_--MX exhibits only a small red shift and almost no saturation at H = 12T, whereas at H = 0, it still saturates, although much less than for σ_--pump. The 1slh–σ_--MX experiences a small but distinct saturation and blue shift with, however, the H = 12T response attenuated as compared to that at H = 0T.

Two sets of effects have to be distinguished, i) the effects of the polarization of the MX's created by the pump (i.e. the difference between the DAS spectra for σ_- and σ_+ excitations), and ii) the effects of magnetic confinement (i.e. the difference between the DAS spectra for H = 0T and H = 12T). The polarization effects can be understood intuitively by considering[9-12]: i) Pauli exclusion and the symmetry of the e and h states out of which the MX's are built, and ii) the "molecular" exciton-exciton interaction potential which is attractive in the singlet state and repulsive in the triplet state. PSF and EXCH are strongly active when the pump and probe MX's involve the same e and/or h states. The sign of the shift experienced by the probe MX's derives from the attractive or

repulsive character of the MX-MX interaction. The evolution of the nonlinear response vs H was briefly discussed above. The combination of these two effects explains that, i) the MX-MX interaction is reduced at high field ii) the shifts of the resonances, while keeping the same sign as for H = 0T, decrease as H increases, iii) the inter-MX dielectric screening itself is strongly attenuated. Screening is often associated with charged e-h plasmas which have a very strong effect because there is no gap in their excitation spectrum. A gas of neutral particles can screen as well. In this case the effect is due to the polarization of the particles, as in the case of molecular gases or dielectric media.[19] The gas of MX's generated by the pump reacts exactly in the same way. Because the MX's excitation spectrum has gaps, this dielectric screening is weaker than that of a charged plasma. Nevertheless it is present and significant at high densities. It explains the important reduction of oscillator strength of the 1shh–σ_--MX seen at H = 0T for the σ_+-pump. As the magnetic field is increased, the MX's wave function is compressed and they become much less polarizable. At very large field, H = 12T, the MX's are almost rigid and their dielectric screening almost disappears Hence the 1shh–σ_--MX's are no more affected by the σ_+-MX's generated by the pump. To more qualitatively characterize the evolution of the MX-MX interaction we have measured the changes of the blue shift of the 1S-MX vs H with linear polarization on another sample and at moderate densities. The variation of the blue shift normalized to the MX-density directly measures the interaction potential. The experimental results for H = 0T, 6T and 12T, are shown in Figure (5). They clearly demonstrate that the shift and hence the XXI tend to zero as H increases. To the best of our knowledge our experiments represent the first confirmation of the remarkable, exact many-body theory results.[7,8,13-15]

To go beyond these qualitative arguments, a time dependent many-body theory of MX-nonlinearities was developed.[10,20] It follows the unrestricted Hartree-Fock theory, introduced by Schmitt-Rink et al.[21], which has been very successful in describing the near band gap nonlinear optical effects in semiconductors.[22-26] In the MX case rather than using the Bloch states as a basis, the MX wavefunctions, $\zeta_{\nu}(r)$, are expanded on the LL orbitals, L_{ν}. The Hartree-Fock theories are more appropriate in this case since they become exact in the extreme magnetic limit, $\lambda \rightarrow \infty$.[7,8] The formalism follows closely that described in our other lecture. Expressed in terms of the optically connected conduction and valence band LL's, which form a set of two-level systems, the density matrix breaks into 2×2 blocks;

$$\hat{n}_{\nu}(t) = \begin{bmatrix} n_{c,\nu}(t) & \psi_{\nu}(t) \\ \psi^{*}_{\nu}(t) & n_{v,\nu}(t) \end{bmatrix}. \tag{3}$$

where $n_{(c,v),\nu}(t)$ are the components of the populations of the conduction and the valence band LL's and $\psi_{\nu}(t)$ are the components of the pair amplitude. The density matrix obeys the Liouville equation. The difference between this model and a collection of independent two-LL systems arises from the coupling between the LL's by the Coulomb interaction, $V_{\nu,\nu'}$. This coupling modifies the physics in two ways. First, the conduction and valence band energies are renormalized by the excited populations in direct analogy with the mechanisms responsible for band gap renormalization,

$$\varepsilon_{j,\nu}(t) \rightarrow \varepsilon_{j,\nu} - \sum_{\nu'} V_{\nu,\nu'} n_{j,\nu'}(t) \tag{4a}$$

(j = e or h). Secondly, the coupling with the electromagnetic field, which is expressed by

the Rabi frequency is modified according to:

$$\mu E(t) \rightarrow \Delta_\nu(t) = \mu E(t) + \sum_{\nu'} V_{\nu,\nu'} \psi_{\nu'}(t). \qquad (4b)$$

This expresses the fact that the optically connected LL's at ν do not experience the applied field, $\mu E(t)$. Rather they see the self-consistent "local field", $\Delta_\nu(t)$, which is the sum of the applied field and the "molecular" field, due to all the other e-h LL's.[10,20] This is the LL-representation of the renormalization which we have expressed in k-space in our other lecture. The interaction between MX's appears in the Liouville equation as an "exchange" term;

$$\sum_{\nu'} V_{\nu,\nu'} [\psi_{\nu'} n_\nu - \psi_\nu n_{\nu'}]. \qquad (5)$$

It is important to note that this term vanishes indentically on the diagonal, $\nu = \nu'$, giving the clue which explains the observed difference in the interaction between MX's in the same state and in different states at low and high magnetic fields. In the Hilbert space, the effect of H can be viewed as a rotation that aligns the MX's along the LL's basis vectors, as we mentioned when discussing the spectra of Figure (1) and (2). For small fields, the MX's have components on many LL's and at large field they have components only on a small subset of LL's. Eventually for $H \rightarrow \infty$ the MX's are exactly aligned with the LL's. Therefore, for a small H there is a strong interaction between all the MX s, through their components on different LL's, L_ν and $L_{\nu'}$, whenever one MX state is photoexcited. At high field, the interaction within one MX state vanishes and yet persists between different MX states. The residual interaction is mostly due to the self-energy corrections, which explain the high field disappearance of the 1s-MX blue-shift found experimentally. The

attractive inter-MX self-energy correction explains the experimental red shift of the 2s-MX induced by a population of photoexcited 1s-MS. At high field MX's behave like two-LL systems and their nonlinear optical response become dominated by Pauli exclusion. Numerical solutions of the Liouville equation reproduce the experimental results fairly well.[10,20] In particular they show that indeed Coulomb correlation is completely quenched in the extreme magnetic limit.

III) Relaxation of electron-hole pairs

An important aspect of a quasi-0D DOS is that the states are lumped together in narrow energy bands as compared to the 1D, 2D and 3D DOS which contain continua. Therefore, for any transition in quasi-0D, the number of available initial and final states is limited. This is expected to strongly influence relaxation and can have important consequences in the dynamics of devices. In this section we discuss how a reduced quasi-0D dimensionality affects the thermalization carrier populations by carrier-carrier scattering. We also discuss nonlinear optical spectroscopy investigations of the relaxation of angular momentum within MX's via transition to one-photon forbbiden states.

Using ≈100fs circular polarized pump pulses, nonthermal populations were generated at about 25meV above the lowest 1shh-resonance of the QW sample at a lattice temperature of 4K. The DOS was controlled by varying the applied magnetic field from H = 0T to H =12T.[11,12] The spin dependent PSF, which determines the energy location of the carriers, was separated from the spin-independent charge density effects as discussed in Section II. The $\sigma\pm$-probe DAS measured for a σ_+-pump is substracted from the $\sigma\pm$-probe DAS measured for a σ_--pump.[11] Figure (6) compares these nonlinear

differential circular dichroism spectra, for two pump/probe delays, Δt = 0fs and 200fs, and for the two cases, H = 0 Figure (6a), and H =12T Figure (6b). In agreement with previous observations,[27,28] in the absence of a magnetic field one observes at Δt = 0 an instantaneous spectral hole burning in the continuum at an energy slightly lower than the pump photon central energy and no response at the 1shh exciton. Hole burning in the continuum is the signature of the PSF induced by the nonthermal populations generated by the pump. At Δt = 200fs the carriers have thermalized by collision among themselves and occupy the states at the bottom of the band, out of which the 1shh-X's and 1slh-X's are made. They thus block the transitions to the X's. Hence the DAS reproduces the profile of these two resonances and the spectral hole in the continuum has disappeared. Because the excess energy is smaller than the energy of optical phonons, the thermalization is internal to the plasma, i.e., the average energy remains constant as the e-h populations *quickly establish a thermal distribution among themselves* at a temperature different from that of the lattice.[28] When the magnetic field is applied, the same pump excites the 2s-MX as shown in the inset of Figure (6b). There is immediately a strong PSF signal at the 2s-MX and a small signal due to dielectric screening at the 1shh-MX and 1slh-MX (note the different scales of the Figure (6a) and (6b)). The important result is that the spectra at Δt = 0fs and Δt = 200fs are almost identical. The nonthermal populations are blocked at 25meV above the lowest states. The inelastic carrier-carrier scattering is quenched because of the limited number of final states available in the quasi-0D DOS. In addition the carriers cannot emit optical phonons because their energy is too small. The confinement in quasi-0D causes a dramatic reduction of the thermalization rates which has, of course, important implications for

device applications.[11,12]

The polarization resolved pump/probe techniques also allow a study of relaxation processes associated with spin. The level diagram of the inset of Figure (2) shows that under magnetic field the lowest energy exciton state, MX_{min} is built up of a |3/2, −3/2> hole and a |1/2, 1/2> electron. This transition, with $\Delta m = 2$, is forbbiden by one photon absorption and therefore it is usually not observed. At H = 12T the MX_{min} is about 1.4meV below the lowest one-photon active MX. It can be generated indirectly, however, from one-photon active MX undergoing a spin-flip of the electron or the hole. This can be the case for the electron spin-flip of the $1S\text{–}MX^{+}_{hh}$, made of a |3/2, −3/2> hole and a |1/2, −1/2> electron, or the hole spin-flip of $1S\text{–}MX^{-}_{hh}$, made of a |3/2, 3/2> hole and a |1/2, 1/2> electron. We have observed such spin relaxation by following the evolution of the DAS measured with a σ_--probe after resonant excitation of the $1S\text{–}MX^{-}_{hh}$ and $1S\text{–}MX^{+}_{hh}$ by σ_--pump and σ_+-pump respectively.[12] The spin relaxation is found to occur on a very long time scale as compared to all the other processes discussed so far. As shown on Figure (7c) it is only after $\Delta t = 200$ps that the two DAS become identical. For shorter delays, Figure (7a) and (7b), the two DAS show very distinct features at the 1S-transition and almost identical profiles at higher energy. This response is in agreement with the discussion of Section II, where we stressed that for 1S resonant excitation the high energy MX's are affected by charge density effects only. Furthermore, it is seen that the DAS profiles of these MX's do not change after $\Delta t \simeq 1$ps. This behavior shows that on the time scale of the experiment, the charge density in the sample is constant after it has been generated. From the exponential decay of the 1S–MS's DAS we infer a time of 65±5ps for flipping angular momentum of the $1S\text{–}MX^{-}_{hh}$ hole and a time of 105±10ps for

flipping the 1S–MX^{+}_{hh} electron. Such long times are consistent with the spin relaxation times which have been reported recently.[29-32] A direct comparison, however, is difficult since we measure the flipping time of an electron or a hole within a MX, whereas the other measurements are relative to the spin flip of free carriers.

IV) Conclusion

We have explored the femtosecond dynamics of the nonlinear optical response of Magneto-excitons, as the quasi-2D quantum well electronic states are further confined in quasi-0D by a strong magnetic field. We have observed, in agreement with the exact many-body theory result, that at high field Coulomb correlation between magneto-excitons in the same state is quenched. It persists, however, between magneto-excitons in different states giving strong nonlinear responses. These results show that a gas of magneto-excitons is a unique two-component many-body system that behaves very differently from the one-component systems such as the fractional Quantum Hall Effect condensate or the Wigner crystal. We have also found that the magnetic field induces a restriction on the number of states available for transition, which almost completely quenches the relaxation of nonthermal populations. This produces qualitatively different carrier dynamics that must be accounted for in any quasi-0D system or device. Finally we have observed relaxation of angular momentum of the electron and hole within magneto-excitons, which results in a transition toward a one-photon forbidden state.

ACKNOWLEGEMENT: This work was performed in collaboration with J.B. Stark, W.H. Knox and S. Schmitt-Rink.

The work of DSC is supported by the Director, Office of Energy Research, Office of

Basic Energy Sciences, Division of Materials Sciences of the US Department of Energy, under Contract No. DE-AC03-76SF00098.

REFERENCES

1. S. Schmitt-Rink, D.S Chemla, D.A.B. Miller, Adv. in Phys. 38, 89 (1989)
2. O. Akimoto, and H. Hasegawa, J. Phys. Soc. Jnp., 22, 181 (1967)
3. M. Shinada, and K. Tanaka, J. Phys. Soc. Jnp., 29,1258 (1970)
4. S.R.E. Yang, and L.J. Sham, Phys. Rev. Lett. 58, 2598 (1987)
5. G.E.W. Bauer, and T. Ando, Phys. Rev. B38, 6015 (1988)
6. H. Chu, and Y.C. Chang, Phys. Rev. B40, 5497 (1989)
7. I.V. Lerner and Yu. E. Lozovik, Zh. Eksp. Teor. Fiz. 80, 1488 (1981) [Sov. Phys. JEPT 53, 763 (1981)]
8. D. Paquet, T.M. Rice, and K. Ueda, Phys. Rev. B32, 5208 (1985)
9. J.B. Stark, W.H. Knox, D.S. Chemla, W. Schäfer, S. Schmitt-Rink and C. Stafford, Phys. Rev. Lett. 65, 3033 (1990)
10. S. Schmitt-Rink, J.B. Stark, W.H. Knox, D.S. Chemla, W. Schäfer, Appl. Phys. A 53, 491 (1991)
11. J.B. Stark, W.H. Knox, D.S. Chemla, Phys. Rev. Lett. 68, 3080 (1992)
12. J.B. Stark, W.H. Knox, D.S. Chemla, Phys. Rev. B46, 7919 (1992-II)
13. A.B. Dzyubenko, and, Yu. E. Lozovik, J. Phys. A24, 415 (1991)
14. V. M. Apalkov and E.I. Rasbha JETP lett.53, 442, (1991).
15. G.E.W. Bauer Phys. Rev. Lett.64, 60 (1990)

16. S. Schmitt-Rink, D.S. Chemla, and D.A.B. Miller, Phys. Rev. B32, 6601 (1985)

17. N. Peyghambarian, H.M. Gibbs, J.L. Jewell, A. Antonetti, A. Migus, D. Hulin, A. Mysyrowicz, Phys. Rev. Lett. 53, 2433 (1984)

18. D. Hulin, A. Mysyrowicz, A. Antonetti, A. Migus, W. T. Masselink, H. Morkoc, H.M. Gibbs, N. Peyghambarian, Phys. Rev. B33, 4389 (1986)

19. H. Haug and S. Schmitt-Rink, Prog. Quant. Electron. 9, 3 (1984)

20. C. Stafford, S. Schmitt-Rink, W. Schäfer, Phys. Rev. B41, 10,000 (1990-I)

21. S. Schmitt-Rink, D.S. Chemla, Phys. Rev. Lett. 57, 2752 (1986). and S. Schmitt-Rink, D.S. Chemla, H. Haug, Phys. Rev. Lett. B37, 941 (1988).

22. W. Schäfer, Adv. Solid State Phys. 28, 63, (1988), W Schäfer, K.H. Schuldt, and R. Binder, Phys. Stat. Sol. B150, 407 (1988)

23. C. Ell, J.F. Muller, K. El Sayed, L. Banyai, and H. Haug, Phys. Stat. Sol. B150, 393 (1988) and Phys. Rev. Lett. 62, 304 (1989)

24. R. Zimmermann, Phys. Stat. Sol. B146, 545 (1988) and R. Zimmermann and M. Hartmann Phys. Stat. Sol. B150, 365 (1989)

25. I. Balslev, R. Zimmermann, and A. Stahl, Phys. Rev B40, 4095 (1989)

26. R. Binder, S.W. Koch, M. Lindberg, N. Peyghambarian, and, W. Schäfer, Phys. Rev. Lett. 65, 899 (1990)

27. W.H. Knox, C. Hirlimann, D.A.B. Miller, J. Shah, D.S. Chemla, and C.V. Shank, Phys. Rev. Lett. 56, 1191 (1986).

28. W.H. Knox, D.S. Chemla, G. Livescu, J.E. Cunningham, and J.E. Henry, Phys. Rev. Lett. 61, 1290 (1988), W.H. Knox, in "Hot Carriers in Semiconductor Nanostructures", J. Shah ed. Academic Press (1992).

29. A. Tackeuchi, S. Muto, T. Inata, T. Fujii, Appl. Phys. Lett. 56, 2213, 1990.

30. M. Kohl, M.R. Freeman, D.D. Awschalom, J.M. Hong, Phys. Rev. B44, 5923, (1991-I)

31. T.C. Damen, L. Viña, J.E. Cummingham, J. Shah, Phys. Rev. Lett. 67, 3432 (1991)

32. S. Bar-Ad, I. Bar-Joseph, Phys. Rev. Lett. 68, 349 (1992)

FIGURE CAPTIONS

Figure 1: Linear absorption of a $L_z = 84$Å GaAs/AlGaAs quantum well structure for σ_- polarized light for a series of magnetic fields H = 0 →12 T.

Figure 2: Comparison of the H = 12 T absorption spectra of the $L_z = 84$Å GaAs/AlGaAs quantum well structure for σ_- (dashed line) and σ_+ (solid line) polarization.
Inset: Schematic of the Γ-point energy levels and one photon interband transitions.

Figure 3: Differential absorption spectra vs photon energy and time delay, Δt, for σ_--probe and (a) σ_--pump, (b) σ_+-pump. The Nonlinear differential circular dichroism spectra (c) are the differences between the spectra (a) and the spectra (b). They reveal the spin-depentent interactions between Magneto-excitons.

Figure 5: Detail of the absorption spectra seen by a σ_--probe near the 1s exciton resonances for Δt = −660fs, 0fs and +660fs and for H = 0T; (a) σ_--pump and (b) σ_+-pump, and for H = 12T; (c) σ_--pump and (d) σ_+-pump.

Figure 6: Evolution of the blue shift of the 1shh exciton normalized to the exciton density vs magnetic field H, for moderate excitation densities.

Figure 7: Circular dichroism spectra, for excitation 25meV above the 1shh resonance and at Δt = 0fs (solid line) and Δt = 200fs (dashed line) for (a) H = 0 and (b) H = 12 T

Figure 8: Differential transmission spectra of a σ_--probe for excitation resonant with the 1S exciton by a σ_--pump (a) and a $\sigma+$-pump (b). In (a) and (b) the spectra correspond to $\Delta t = 0.66$ps (solid line), 40.66ps (dotted line) and 66.66ps (dash-dotted line). After $\Delta t = 200$ps the spectra become identical (c).

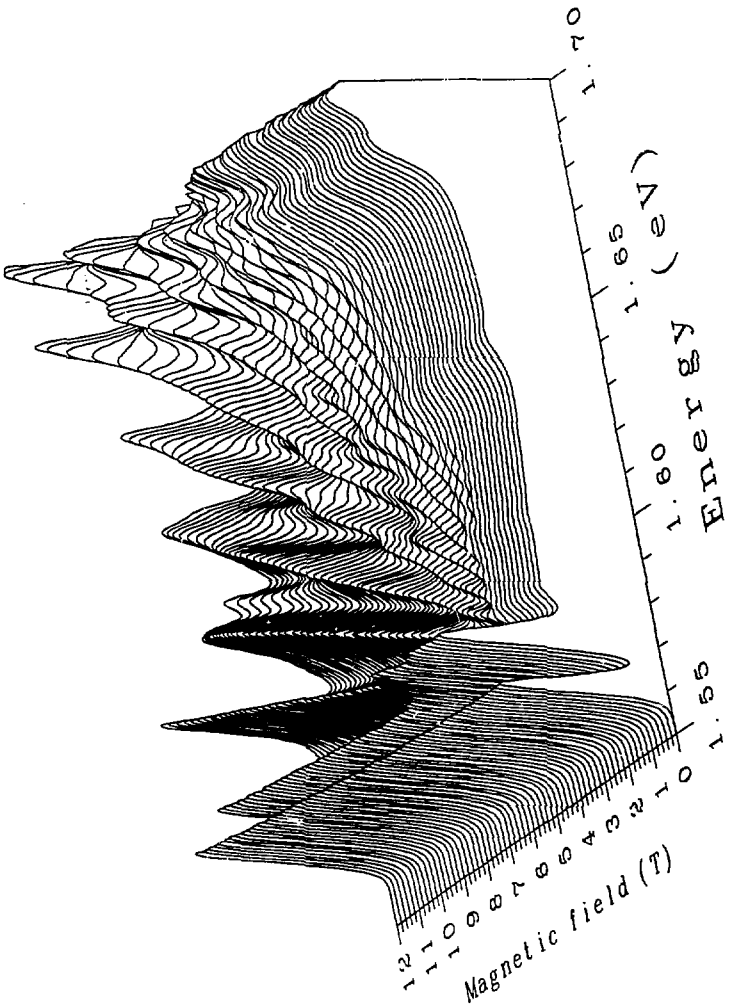
Magnetic field (T)
12
11
10
9
8
7
6
5
4
3
2
1
0
1.55
1.60
1.65
1.70
Energy (eV)

XBL 926-1427

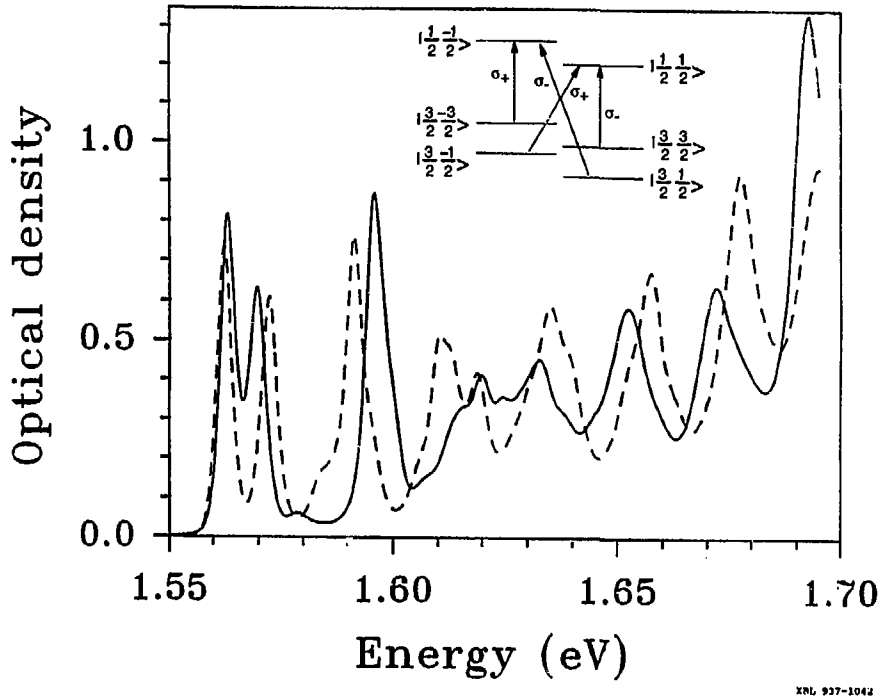
Optical density
1.0
0.5
0.0
1.55
1.60
1.65
1.70
Energy (eV)
$|\frac{1}{2}\frac{-1}{2}\rangle$
$|\frac{3}{2}\frac{-3}{2}\rangle$
$|\frac{3}{2}\frac{-1}{2}\rangle$
$|\frac{1}{2}\frac{1}{2}\rangle$
$|\frac{3}{2}\frac{3}{2}\rangle$
$|\frac{3}{2}\frac{1}{2}\rangle$
σ_+
σ_-
σ_+
σ_-
XBL 937-1042

(a)
(b)
(c)
Time delay (fs)
Energy (eV)
Circular dichroism
XBL 926-1428

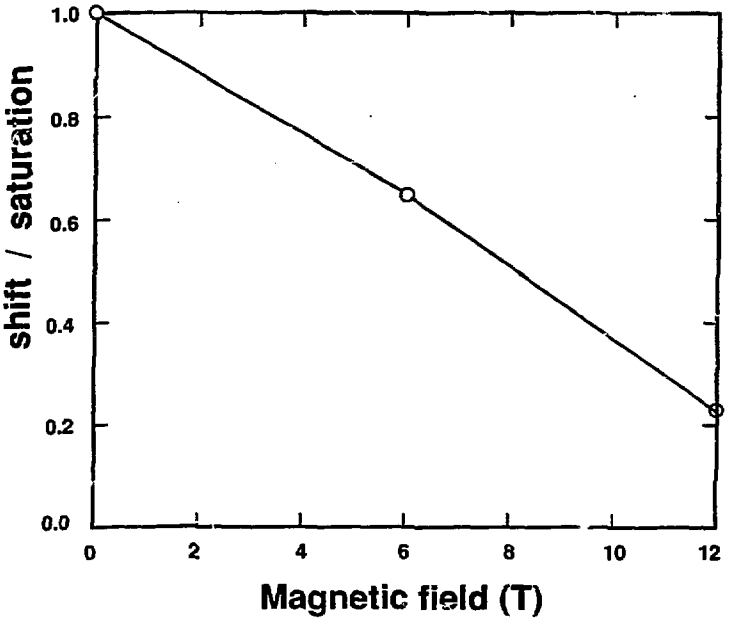
shift / saturation
1.0
0.8
0.6
0.4
0.2
0.0
0
2
4
6
8
10
12
Magnetic field (T)

XBL 928-1912

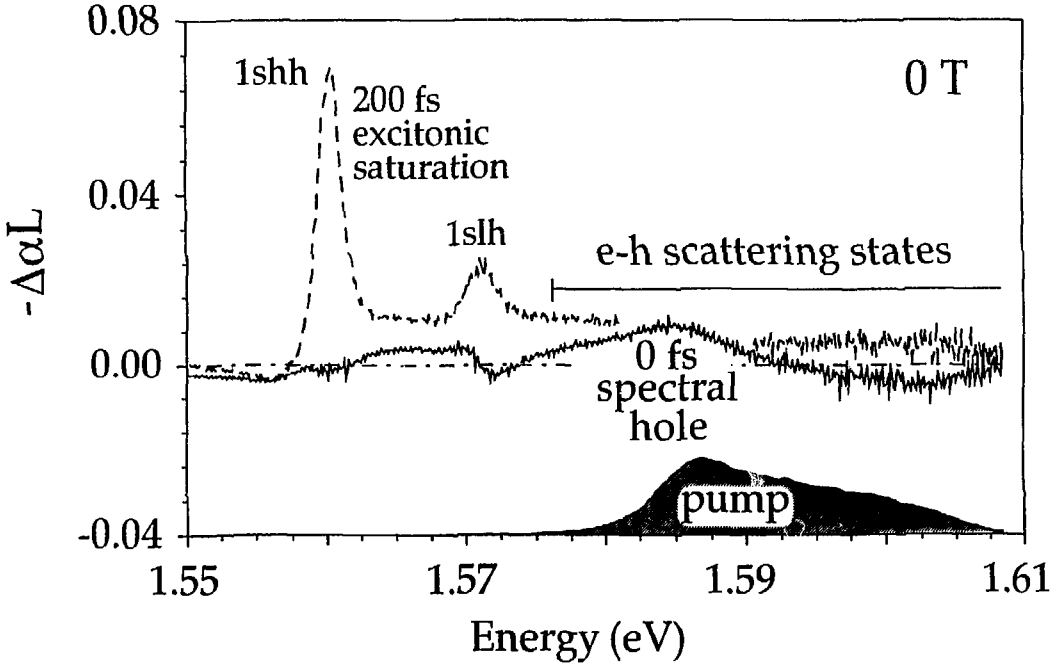
0.08
0.04
0.00
-0.04
-ΔαL
1shh
200 fs
excitonic
saturation
1slh
0 T
e-h scattering states
0 fs
spectral
hole
pump
1.55
1.57
1.59
1.61
Energy (eV)

XBL 926-1429

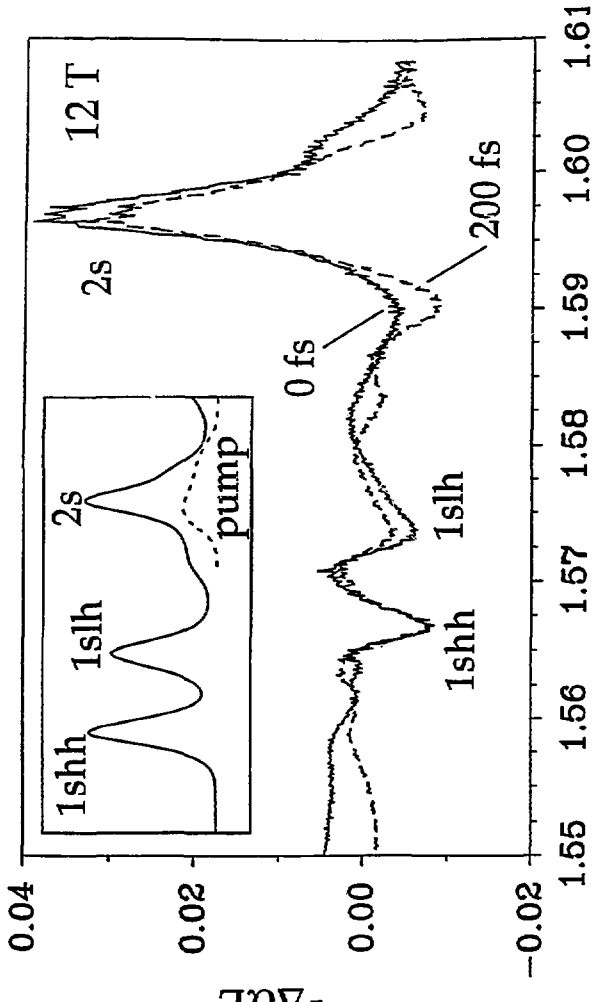
-ΔαL
0.04
0.02
0.00
−0.02
1.55
1.56
1.57
1.58
1.59
1.60
1.61
Energy (eV)
12 T
2s
0 fs
200 fs
1shh
1slh
1shh
1slh
2s
pump
XBL 928-1907

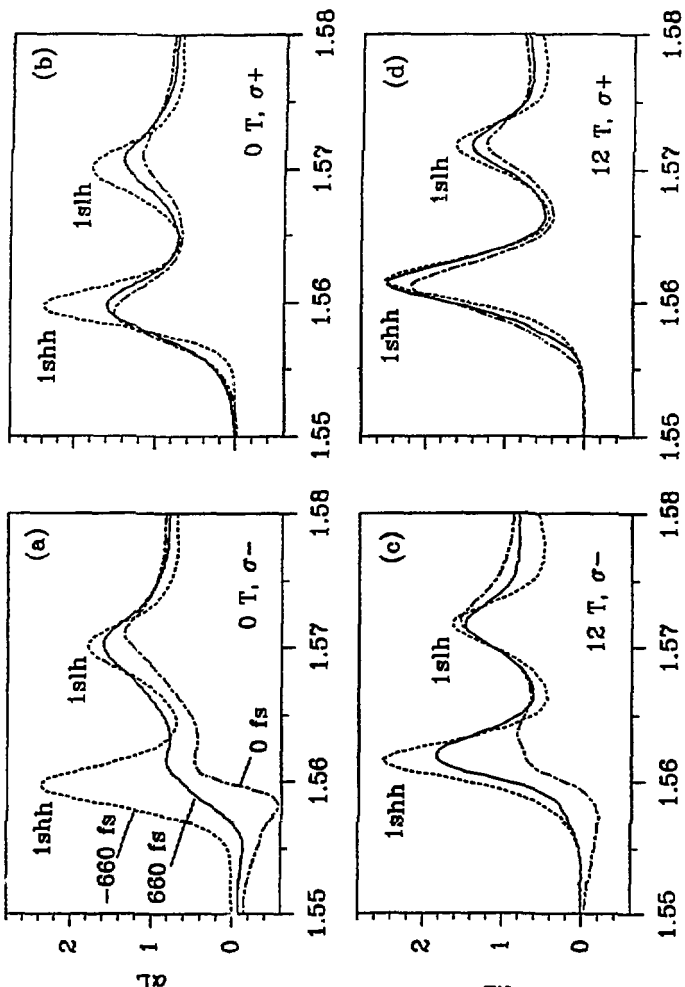
(a)
(b)
(c)
(d)
1shh
1slh
-660 fs
660 fs
0 fs
0 T, σ−
0 T, σ+
12 T, σ−
12 T, σ+
αL
Energy (eV)
XBL 928-1908

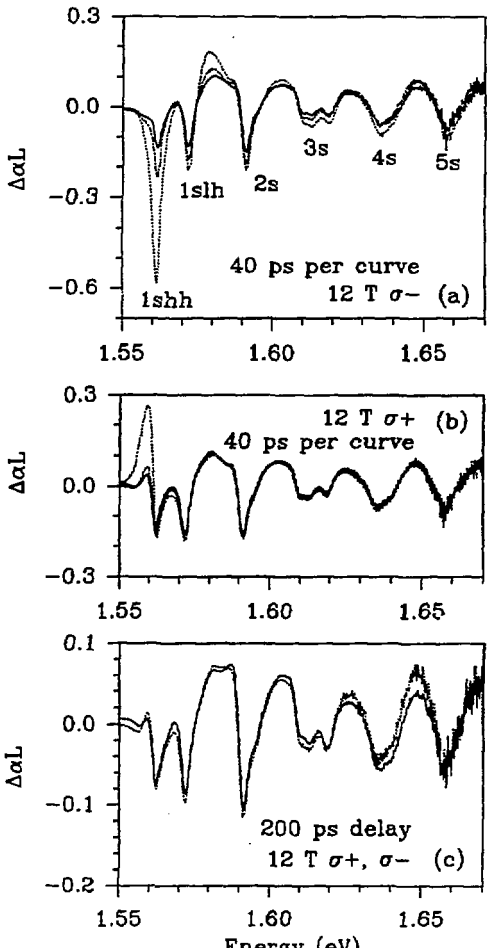
0.3
0.0
−0.3
−0.6
ΔαL
1shh
1slh
2s
3s
4s
5s
40 ps per curve
12 T σ− (a)
1.55
1.60
1.65
0.3
0.0
−0.3
ΔαL
12 T σ+ (b)
40 ps per curve
1.55
1.60
1.65
0.1
0.0
−0.1
−0.2
ΔαL
200 ps delay
12 T σ+, σ− (c)
1.55
1.60
1.65
Energy (eV)

XBL 936-1032